Proceedings of the 28th Conference
on Decision and Control
Tampa, Florida • December 1989

PERFORMANCE OF MAXIMUM–LIKELIHOOD DECONVOLUTION FOR BERNOULLI–GAUSSIAN PROCESSES

Chong–Yung Chi

Department of Electrical Engineering
National Tsing Hua University
Hsinchu, Taiwan, Republic of China

ABSTRACT

In this paper, we propose a performance analysis regarding false alarms, correct detections and the resolution for the well–known maximum–likelihood deconvolution (MLD) for Bernoulli–Gaussian (B–G) processes distorted by a linear time invariant system. We also show some simulation results using synthetic data which support the proposed analysis.

I. INTRODUCTION

Estimation of a desired signal $\mu(k)$, which is distorted by a linear time–invariant system $v(k)$, from noisy measurements, $z(k)$, $k=1,2,...,N$, where

$$z(k) = \mu(k) * v(k) + n(k) \qquad (1)$$

where $n(k)$ is the measurement noise, is a deconvolution problem which can be found in seismology, biomedical ultrasonic imaging and channel equalization. The well–known prediction error filter [1] has been used in seismic deconvolution about three decades. In the past decade, Kormylo and Mendel [2,3] proposed a B–G model for a sparse spike sequence $\mu(k)$ as follows:

$$\mu(k) = r(k)\, q(k) \qquad (2)$$

where $r(k)$ is a white gaussian random process with zero mean and variance σ_r^2 and $q(k)$ is a Bernoulli process defined as

$$P_r[q(k)] = \lambda^{q(k)}\,(1-\lambda)^{(1-q(k))} \qquad (3)$$

where $q(k)$ can take only a binary value one or zero and $0\leq\lambda\leq 1$ is the probability for $q(k)$ equal to 1. Kormylo and Mendel [2,3] developed an MLD based on this model and the assumption that $n(k)$ is white gaussian with zero mean and variance σ_n^2.

In this paper, we present, in addition to SNR, what characteristics of $v(k)$ determine the performance of the MLD algorithm. For simplicity, we assume that statistical parameters λ, σ_n^2, σ_r^2 and $v(k)$ are given a priori and present a performance analysis for the estimation of $\mu(k)$.

II. BACKGROUND OF ML DECONVOLUTION

The MLD tries to search for the $q(k)$ such that the likelihood defined as

$$S\{\underline{q}|\underline{z}\}=p(\underline{z},\underline{q}) \qquad (4)$$

is maximum, where $\underline{z} = (z(1),z(2), \cdots,z(N))'$ and $\underline{q} = (q(1),q(2), \cdots,q(N))'$. The optimal ML solution for $q(k)$ is never implemented in practice because far too many possible $q(k)$'s need to be tested. Therefore, the following performance analysis is associated with a well–known suboptimal ML algorithm, called single–most–likely–replacement (SMLR) [1,2] algorithm, which iteratively updates a reference sequence $\underline{q}_r$ by $\underline{q}_{k'}$ until convergence where $q_k(i) = q_r(i)\,[1-\delta(i-k)] + [1-q_r(i)]\,\delta(i-k)$ and k' is associated with the maximum of the likelihood ratio $\Lambda(k,\underline{q}_r) = S\{\underline{q}_k|\underline{z}\}/S\{\underline{q}_r|\underline{z}\}$. After detection of $q(k)$, $r_{ML}(k)$ can be obtained using the minimum–variance deconvolution filter [3].

III. PERFORMANCE ANALYSIS

The performance of the SMLR detector can be predicted from the value of $P_r(k')$. However, the derivation of $P_r(k')$ is almost formidable if not impossible. Therefore, the following analysis is based on a heuristic assumption that $P_r(k')$ is proportional to the mean value, $E[\ln\Lambda(k',\underline{q}_r)]$, of $\ln\Lambda(k',\underline{q}_r)$, which is then computable and is a function of both SNR and wavelet characteristics. We use it to analyze the dependence of $P_r(k')$ upon both SNR and wavelet characteristics.

The true $q(k)$, denoted $q_T(k)$, for a small λ is a sparse spike train which is basically composed of isolated single spikes and pairs of two close spikes. Various aspects of performance including false alarms, correct detections and the resolution can be unravelled by considering the following two cases.

CASE I. $q_T(k) = \delta(k-k_1)$:

Different selections of $\underline{q}_r$ will lead to different aspects of the performance. We consider three selections of $\underline{q}_r$ as follows:

I–A. $q_r(k) = 0$, no spikes in $\underline{q}_r$;

I–B. $q_r(k)=\delta(k-k_1)=q_T(k)$;

I–C. $q_r(k)=\delta(k-m)$, $m\neq k_1$, a false alarm in $\underline{q}_r$.

We only present the analysis for case **I–A**. The analysis for the other two cases can be similarly performed. For this case, it can be shown that

$$E[\ln\Lambda(k,\underline{q}_r)]\cong -\frac{1}{2} + \frac{F}{2}\,\gamma^2(k-k_1) - \frac{\ln F}{2} + \ln\frac{\lambda}{1-\lambda} \qquad (5)$$

where $F=SNR/\lambda$, and $\gamma(k)=\varphi(k)/\varphi(0)$ and $\varphi(k)=v(k)*v(-k)$. Note that $\gamma(0)=1$, $\gamma(k)=\gamma(-k)$ and $|\gamma(k)|\leq 1$. Let us consider all possible cases about k' as follows:

(I–A–1) $k'=k_1$, a correct detection occurs;

(I–A–2) $k'\neq k_1$, a false alarm occurs.

One can see, from (5), that $\max\{\ln\Lambda(k,\underline{q}_r)\} = \ln\Lambda(k_1,\underline{q}_r)$ and $\Delta(k) = \max\{\ln\Lambda(k,\underline{q}_r)\} - \ln\Lambda(k,\underline{q}_r) =(F/2)[1-\gamma^2(k-k_1)]$. We now infer $P_r(I–A–1) = P_r(k'=k_1)$ and $P_r(I–A–2) = P_r(k'\neq k_1)$ from $\Delta(k)$. $P_r(I–A–1) - P_r(I–A–2)$ increases as F increases and $\gamma^2(k)$ decreases, but has nothing to do with the length of $\gamma(k)$, which is about twice the length of $v(k)$. When $\gamma^2(k)<<1$ for $k\neq 0$ (like a thumbtack), $P_r(I–A–1) >> P_r(I–A–2)$ always happen even when F is not large. However, when $\gamma^2(k)\approx 1$, $|k|\leq W$, for some W, $P_r(I–A–2) > P_r(I–A–1)$ could happen when F is not large. In other words, a false alarm could occur near k_1 when the mainlobe of $\gamma(k)$ is narrow and F is not large. Finally, the ratio $P_r(I–A–1)/P_r(I–A–2)$ can be made arbitrarily large by increasing F or SNR. Therefore, we conclude that the performance is better for larger F and $\gamma(k)$ with a narrower mainlobe.

We draw the following conclusions from the analysis for CASE I inculding **I–A**, **I–B** and **I–C**:

(R1) The performance is better for larger SNR and $\gamma(k)$ with a narrower mainlobe;

(R2) The performance is not dependent upon the wavelet length;

(R3) The performance can be infinitely improved by increasing SNR no matter whether the mainlobe of $\gamma(k)$ is broad or narrow;

(R4) Although false alarms for $\gamma(k)$ with a broad mainlobe cannot be removed by increasing SNR, their amplitudes tend to be smaller for larger SNR;

(R5) For the same performance, a higher SNR is required for $\gamma(k)$ with a broad mainlobe than for $\gamma(k)$ with a narrow mainlobe.

CASE II. $q_T(k)=\delta(k-k_1)+\delta(k-k_2)$, $k_2\neq k_1$:

The analysis for this case is similar to that for CASE I. After we analyzed the following three selections of $\underline{q}_r$:

II–A. $q_r(k)=0$, no spikes in $\underline{q}_r$;

II–B. $q_r(k)=\delta(k-k_1)$, a true spike in $\underline{q}_r$;

II–C. $q_r(k)=\delta(k-m)$, $m \neq k_1$, $m \neq k_2$, a false alarm at k=m.

We ended up with the same conclusions given by (R1) through (R5) for CASE I and one extra conclusion:
(R6) The resolution is better for $\gamma(k)$ with a narrower mainlobe.

IV. SIMULATION EXAMPLES

We select two different wavelets. $v_1(k)$ taken from [1,2] and $v_2(k)$ are shown in Figure 1a. Normalized correlation functions $\gamma_1(k)$ and $\gamma_2(k)$ are shown in Figure 1b.

From Figure 2 where SNR=10, we see that the deconvolved results are very good. These results are consistent with (R1) and (R6) since the mainlobe of $\gamma_1(k)$ is narrow.

Next, let us compare Figure 2 with Figure 3a where SNR=10 and wavelet lengths are about the same for both but the mainlobe widths of $\gamma_1(k)$ and $\gamma_2(k)$ are very different. Obviously, the results shown in Figure 2 are much better than those shown in Figure 3a. This is consistent with (R1) and (R2).

Next, we show the performance improvement for the example associated with $v_2(k)$ by increasing SNR. Figures 3b shows the deconvolved results for SNR equal to 10000. The results shown in this figure are consistent with (R3) and (R4).

Finally, comparing Figure 2 where SNR=10 with Figure 3b where SNR=10000, we see that their performances are comparable but SNR's are very different. This is also consistent with (R5).

V. CONCLUSIONS

In this paper, we have presented an analysis for the performance of a typical suboptimal MLD algorithm, the SMLR algorithm, for B–G processes assuming that statistical parameters λ, σ_r^2 and σ_n^2 and v(k) were given a priori.

The presented analysis led to six main conclusions (R1) through (R6) given in Section III with regard to the dependence of the performance of the SMLR algorithm upon both SNR and the mainlobe width of the normalized autocorrelation function $\gamma(k)$ of v(k). We believe that these conclusions should also apply to other comparable suboptimal ML algorithms and that this analysis can help users explain the deconvolved data from the view points of both SNR and $\gamma(k)$.

REFERENCES

[1] E. A. Robinson and S. Treitel, Geophysical signal analysis, Prentice Hall, Englewood Cliffs, New Jersey, 1980.

[2] J. Kormylo and Jerry M. Mendel, "Maximum–likelihood deconvolution," IEEE Trans. Geoscience and Remote Sensing, vol. GE–21, pp. 72–82, 1983.

[3] J. Mendel, Optimal seismic deconvolution: an estimation–based, Academic Press, New York, 1983.

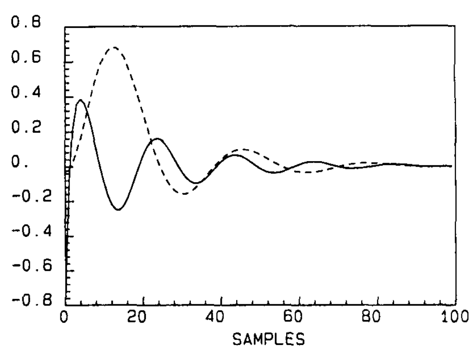

(a)

(b)

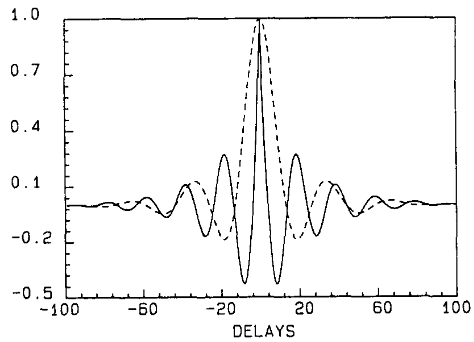

Figure 1 (a) $v_1(k)$ (solid line) and $v_2(k)$ (dashed line) and (b) normalized autocorrelations $\gamma_1(k)$ (solid line) and $\gamma_2(k)$ (dashed line).

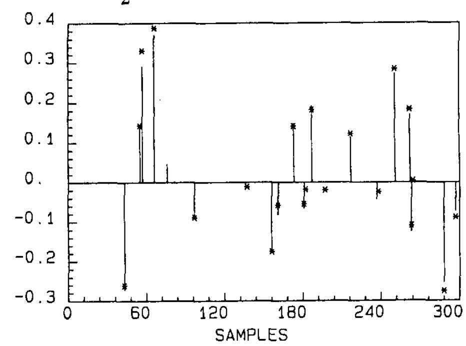

Figure 2 Deconvolved results associated with $v_1(k)$ and SNR=10. *'s denote true spikes and bars denote estimates.

(a)

(b)

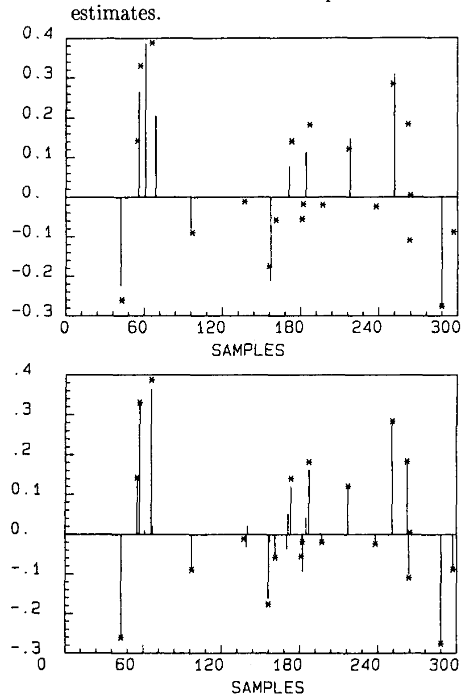

Figure 3 Deconvolved results associated with $v_2(k)$ and (a) SNR=10, (b) SNR=10000, respectively. *'s denote true spikes and bars denote estimates.